

RRScell method for automated single-cell profiling of multiplexed immunofluorescence cancer tissue

Alvason Zhenhua Li, Karsten Eichholz, Anton Sholukh,
Daniel Stone, Michelle Loprieno, Keith Jerome, Khamson Phasouk, Kurt Diem, Jia Zhu, Lawrence Corey

Vaccine and Infectious Disease Division, Fred Hutchinson Cancer Research Center
Seattle, WA 98109, USA

alvali@fredhutch.org

Abstract

Multiplexed immuno-fluorescence tissue imaging, allowing simultaneous detection of molecular properties of cells, is an essential tool for characterizing the complex cellular mechanisms in translational research and clinical practice. New image analysis approaches are needed because tissue section stained with a mixture of protein, DNA and RNA biomarkers are introducing various complexities, including spurious edges due to fluorescent staining artifacts between touching or overlapping cells. We have developed the RRScell method harnessing the stochastic random-reaction-seed (RRS) algorithm and deep neural learning U-net to extract single-cell resolution profiling-map of gene expression over a million cells tissue section accurately and automatically. Furthermore, with the use of manifold learning technique UMAP for cell phenotype cluster analysis, the AI-driven RRScell has equipped with a marker-based image cytometry analysis tool (markerUMAP) in quantifying spatial distribution of cell phenotypes from tissue images with a mixture of biomarkers. The results achieved in this study suggest that RRScell provides a robust enough way for extracting cytometric single cell morphology as well as biomarker content in various tissue types, while the build-in markerUMAP tool secures the efficiency of dimension reduction, making it viable as a general tool in the spatial analysis of high dimensional tissue image.

1. Introduction

Immuno-fluorescent staining is widely used in biomedical research to visualize particular cellular events by specific molecular markers, such as protein-based immunohistochemistry (IHC), and DNA/RNA-based in situ hybridization (ISH). Recent advances in multiplexed IHC/ISH tissue imaging techniques, allowing simultaneous detec-

tion of numerous markers, raise the possibility of conducting deeper immune response profiling at a single-cell level [13, 4].

This growing field reveals a wealth of information about the relationships among cells in the entire tissue micro-environment but presents a significant image analysis challenges. For instance, the membrane-image quality defection due to the immuno-staining techniques is common and significant. Noises bring obstacles to edge detection because it reduces the contrast of real membrane boundary and also introduce spurious edges due to noisy contrast. Furthermore, complex tissue involved in diverse physiological processes, no single technique can provide all of the answers, so it's necessary to use a combination of IHC and ISH methods to providing insights into physiological processes and disease pathogenesis, wherein a mixture of protein, DNA and RNA markers is introducing various complexities. Thus, the multiplexed image-based transcriptional profiling of cells is significant challenging. The cutting edge machine-learning approaches are the promising way to address the challenges.

1.1. Problems and Contributions

The major drawback of supervised machine-learning techniques is that the quality of the results depends upon the amounts and quality of manually annotated training data. However, the performance of human annotators show a high degrees of variability in complex fluorescent image in tissue as shown in Figure 1(C). Furthermore, there is existing gold standard paradox in biomedical tissue [1], so that, it is not practical using manual annotation to generate the consensus ground truth in complex tissue image.

In this work, we aim to solve the practical problem of lacking ground-truth in microscopy tissue image, we have harnessed the stochastic random-reaction-seed (RRS) algorithm as a ground-truth generator. Then, we build a AI-driven pipeline U-net to extract single-cell level informa-

tion from complex tissue. Finally, we address the practical problem of large amounts of single-cell data output from the machine-learning pipeline, demonstrate the simple cost-efficient approach to leverage the power of UMAP (Uniform Manifold Approximation and Projection) [8].

Specifically, the main contributions are as the following: (1) We have designed a RRS-based automated ground-truth generator for training the neural networks, and importantly, the fine-tuned parameters of RRS ensured the generation of a high-quality ground-truth for microscopy image segmentation. (2) We have developed an automated RRScell pipeline for extracting single-cell level profiling map of whole slide tissue. It is a robust convolutional network in biomedical image segmentation with limited training dataset. (3) RRScell has a build-in markerUMAP tool secures the efficiency of dimension reduction, making it viable as a general tool in the spatial analysis of high dimensional tissue image.

1.2. Related Works

Recent advances in machine-learning have outperformed the state of the art of traditional image analysis in many applications. Supervised learning segmentation approaches require abundant ground-truth labels to deliver accurate inference. However, in biomedical microscopy image segmentation, these labor-intensive annotation are scarce [6]. Among various deep convolutional encoder-decoder networks for image segmentation, the U-net is considered a generic architecture in biomedical cell segmentation [9, 5] because data-augmentation strategy in U-net is able to achieve desired accuracy with a few of ground-truth annotation. There has been considerable efforts in computational multiplexed tissue image analysis, some are commercial microscopy platforms or licensed software [3, 13], so they are not easy to be understood, and customized for complex tissues. some are implemented in Matlab or Python wrapper for Matlab, and applied probability maps of nuclei/membrane for generating segmentation ground-truth masks [10, 3, 11]. Many existing multiplexed analysis pipelines are developed for specific assays or certain IHC/ISH schemes, there are lacking consensus standards for individual labs' bespoke IHC/ISH scheme. Image-based cytometry involves a wide range of cutting-edge techniques, more efforts are needed to overcome various issues and limitations in this active research field.

2. Methods

2.1. Automated ground truth generator

We have applied the stochastic RRS method [7] to generate high quality ground-truth automatically, as shown in Figure 1(E). The accuracy of automated ground-truth from RRS is ensured by handcraft parameters for selected im-

age dataset. There is no objective ground truth available for multiplexed immunofluorescence images. To assess the accuracy of our method we compare the results with the manual measurement. As demonstrated in Figure 2(E), the accuracy of RRScell method is equivalent to manual annotation. Furthermore, due to DAPI straining defect in high intensity zone beyond human visual approach, so that both experts are avoiding these messy areas, as shown in Figure 2(C, D), one significant advantages of RRScell is able to tracing more cells based on its powerful combination of both membrane and nuclei as detection, as shown in Figure 2(B). The correct detection of cellular membrane is verified by the nuclei plot in Figure 2(A). As shown in Figure 2(E), the polar plot of bar-chart, where the polar axis is the similarity score, the blue-color bars are corresponding to the cells (blue dots) in the blue box-plot while the green-color bars are corresponding to the cells (green dots) in the green box-plot. In order to demonstrate the variability of manual annotations, the blue-color bars are sorted in descending order, and then the green-color bar is placed by tracking the similar cellular physical location. So that the similarity of each cell annotated by two experts are displayed in a contrast way. The similarity score of each cell membrane profile is calculated by the IoU (intersection over union). Automated RRS-based ground truth generator is accurate and consistent.

2.2. RRScell pipeline

We have built an artificial intelligence (AI)-driven pipeline which is composed of the following modules: (1) Automated cell segmentation is a U-net-based encoder-decoder network with RRS-based ground-truth generator. The cell segmentation is either based on raw membrane staining or anchored to synthetic/artificial membrane from raw nuclei staining/other suitable staining. (2) Automated cell-type detection: As shown in Figure 3, we have developed a workflow for phenotype validation cell-by-cell.

2.2.1 markerUMAP

We have developed a marker-based image cytometry analysis tool (markerUMAP) in quantifying spatial distribution of cell phenotypes from tissue images with a mixture of biomarkers. The strategy of markerUMAP is introducing simplified symbolic marker to represent the captured biomarker contents. For example, the quantification of RNAscope measurement is focused on the detective RNA dot-like distribution instead of normal intensity measurement (since RNA staining enables specific and sensitive detection of RNA, which can be visualized as a dot, with each dot denotes a single RNA transcript). This symbolic marker-based strategy is organically compatible and consistent with UMAP fast, robust and meaningful organization of

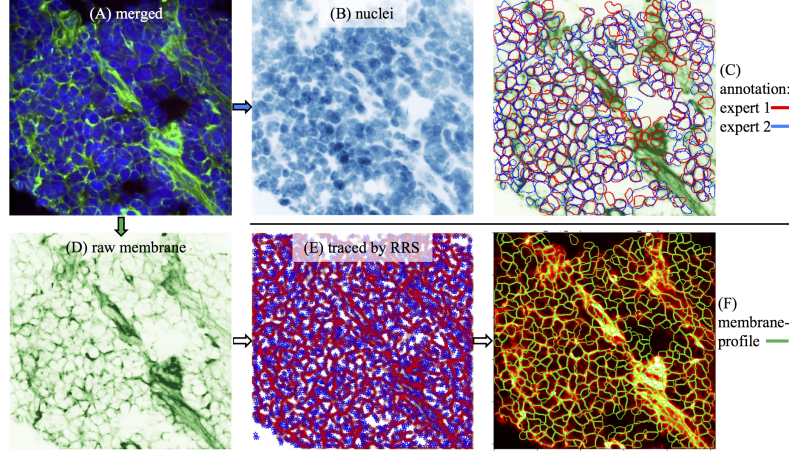


Figure 1. Automated ground truth generation in a sample image from cancer tissue. (A) is the merged image of multiplexed. (B) is raw nuclei channel. (C) are the membrane annotations from two experts (red color from one expert, blue color from another expert) on the same membrane image. (D) is the raw nuclei channel. (E) is the dynamic tracing map on the membrane image by the Random-Reaction-Seed method, where the random initial seed is denoted by blue star, the search chain is denoted by red-circle. [7]. (F) is the traced membrane profile by RRS, the green-color is the traced membrane plotted on the raw membrane image (hot-color-map).

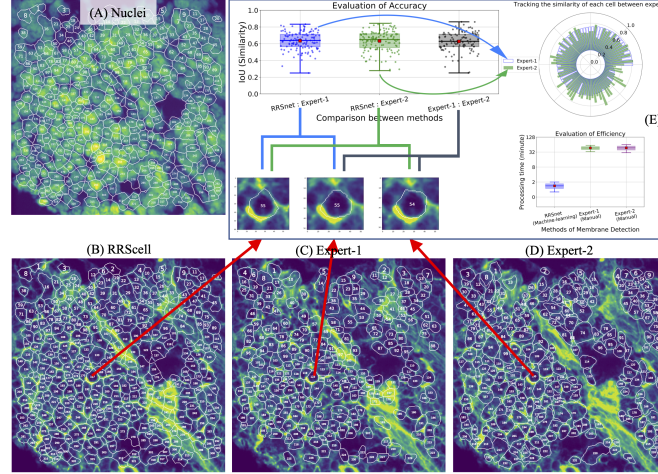


Figure 2. Performance of RRScell method. (A) Membrane profile from RRScell is plotted on the nuclei image. (B) Membrane profile from RRScell is plotted on the membrane image. (C) Manual membrane profile from Expert-1 is plotted on the membrane image. (D) Manual membrane profile from Expert-2 is plotted on the membrane image. (E) The box-plot on the top is the evaluation of accuracy among three different methods, the red-square-point inside each box is the mean value. Comparison between membrane-detection methods: the blue-color box is the similarity between RRScell and expert-1, the blue-color box is the similarity between RRScell and expert-2, the black-color box is the similarity between two experts. The polar plot bar-chart on the upper-right is the evaluation of similarity of each cell between experts: each blue-color bar is corresponding to each dot in the blue-color box-plot, here, the bars are sorted in descending order. The box-plot on the lower-right is the evaluation of efficiency, the efficiency of RRScell is significantly better than the manual process (30 folds difference in processing time).

cell clusters [2].

3. Experiments and Results

In this section, we applied RRScell into multiplexed tissue stained by various IHC/ISH schemes: starting from 3-plex to higher plexed immuno-fluorescence tissues in a gradual way.

3.1. Three-plex CRISPR-Cas9 tissue images without membrane staining

In some practical translational research, multiplexed immunofluorescence tissue images are lacking membrane staining in many circumstances. Therefore, the RRScell pipeline is also equipped with the synthetic/artificial membrane generation step to work flexibly and consistently on membrane-less images. As shown in Figure 4, this

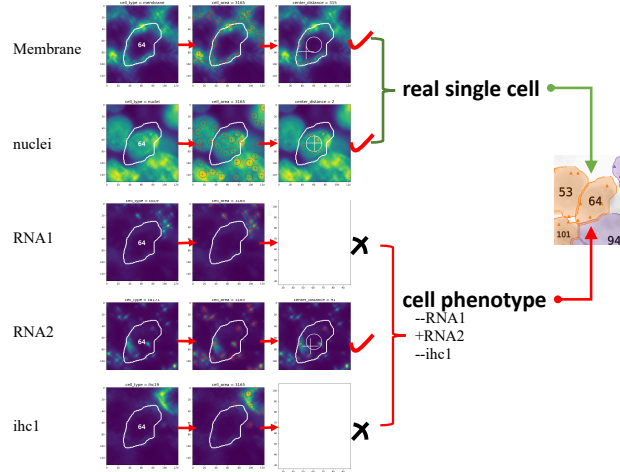


Figure 3. Scheme of automated cell phenotype detection. Here, an example of 5-plex image is presented: the initial step is the validation of real single cell based on both membrane and nuclei features, and a phenotype detection step will be followed in staining conditions (such as RNA1, RNA2, and IHC1).

immuno-fluorescent tissue image is from HBV-specific SaCas9 therapy [12].

3.2. Four-plex CAR-T RNA-scope tissue images with membrane staining

Chimeric antigen receptor (CAR) T cells, as one of rapid emerging form of genetically engineered “artificial immune cell”, have outstanding therapeutic potential for treating cancers [4]. To study the anti-HIV CAR T cell trafficking into tissues with viral replication by microscopy, we developed an RNAscope- based RNA fluorescent in situ hybridization assay. In order to validate the RNA probes, we need to quantify a large volume of image dataset from in vitro culture and tissues sections among mouse, monkey, and human. However, the membrane-image quality defec-tion due to the sugar-staining techniques is common and significant. Noises bring obstacles to edge detection be-cause it reduces the contrast of real membrane boundary and also introduce spurious edges due to noisy contrast, as shown in Figure 6.

3.3. Seven-plex cancer tissue images without mem-brane staining

We are applied ChipCytometry platform for making highly multiplexed assay and imaging on cancer tissues. For higher multiplexed tissue, the potential total cell-phenotypes is in a exponential-growth pattern. For instance, there are total 34 cell-phenotypes are classified in a small corner of 7-plex tissue, as shown in Figure 7. Signifi-cantly, the markerUMAP is able to provide the fast run times, high reproducibility and the meaningful organization of cell-phenotype clusters, as shown in Figure 8.

4. Conclusion

We present a robust, open-source Python pipeline for im-mune cell profiling in spurious-edge-tissues of translational medical research. This machine-learning solution builds upon RRS automated ground truth generation. The house-made automated machine learning pipeline is automatic scaling up from 3 to 7, or highly multiplexed immuno-fluorescent tissue images. The AI-driven RRScell method has demonstrated the robustness and flexibility for single-cell profiling of various tissue types and formats where membrane and nuclei are often missed.

In conclusion, RRScell, as a framework combining HMM-based (hidden-Markov-model) RRS, deep neural learning network U-net, and manifold learning technique UMAP, has demonstrated the effectiveness and robustness for precise quantification of immune cell phenotypes in images taken from noisy multiplexed immunofluorescence cancer tissue, which is becoming an increasingly useful tool for biomedical researches owing to its ability to profiling cellular phenotyping in cancer resection tissues with various complexities. Furthermore, the markerUMAP image-based cytometry tool inside RRScell has emerged as promising spatial analysis tool in ongoing high-dimensional immuno-straining tissues in pre-clinical research and clinical trials.

References

- [1] Famke Aeffner, Kristin Wilson, Nathan T. Martin, Joshua C. Black, Cris L. Luengo Hendriks, Brad Bolon, Daniel G. Rud-mann, Roberto Gianani, Sally R. Koegler, Joseph Krueger, and G. Dave Young. The gold standard paradox in dig-ital image analysis: Manual versus automated scoring as ground truth. *Archives of Pathology & Laboratory Medicine*, 141(9):1267–1275, 2019/12/08 2017.

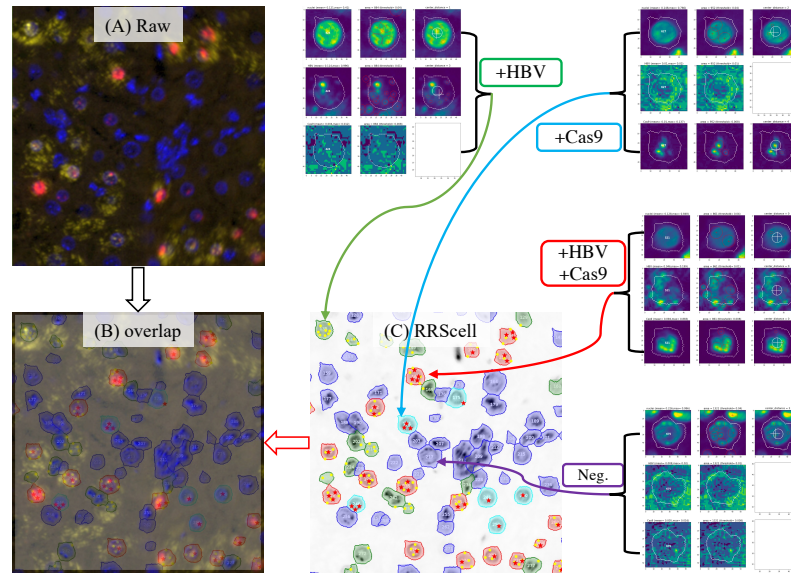


Figure 4. RRSCell phenotype detection of 3-plex immuno-fluorescent tissue image from HBV-specific SaCas9 therapy. (A) is the raw image of 3 channels: red color denotes the Cas9 RNA-staining, yellow color denotes the HBV RNA-staining, and blue color denotes the nuclei staining. (B) is given the overlapped image from the raw and the RRSCell profiling map. (C) is profiling map from the cell phenotype analysis by the RRSCell pipeline: detected +HBV dots are denoted by yellow-disk, detected +Cas9 dots are denoted by red-star. There are four types of cells: +HBV, +Cas9, +HBV+Cas9, and negative -HBV-Cas9.

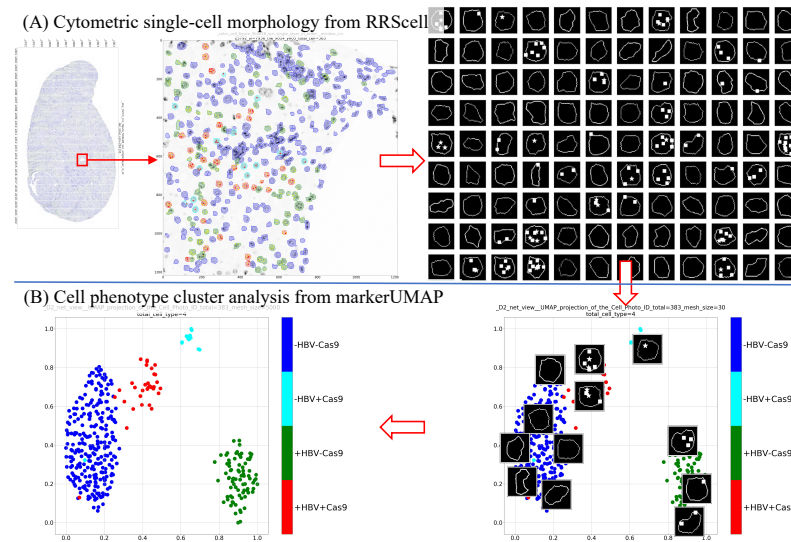


Figure 5. makerUMAP phenotype clustering analysis of 3-plex immuno-fluorescent tissue image from HBV-specific SaCas9 therapy. (A) Demonstration of extracting single-cell level information from individual cells in whole slide tissue by RRSCell. (B) Demonstration of cell phenotype cluster analysis by markerUMAP tool. Note: only a small part of the tissue was applied in this demonstration.

- [2] Etienne Becht, Leland McInnes, John Healy, Charles-Antoine Dutertre, Immanuel W H Kwok, Lai Guan Ng, Florent Ginhoux, and Evan W Newell. Dimensionality reduction for visualizing single-cell data using umap. *Nature Biotechnology*, 37(1):38–44, 2019.
- [3] Eric Czech, Bulent Arman Aksoy, Pinar Aksoy, and Jeff Hammerbacher. Cytokit: a single-cell analysis toolkit for high dimensional fluorescent microscopy imaging. *BMC*

- Bioinformatics*, 20(1):448, 2019.
- [4] Karsten Eichholz, Alvason Zhenhua Li, Kurt Diem, Michael C. Jensen, Jia Zhu, and Lawrence Corey. A carna fish assay to study functional and spatial heterogeneity of chimeric antigen receptor t cells in tissue. *bioRxiv*, page 2020.08.21.260935, 01 2021.
- [5] Thorsten Falk, Dominic Mai, Robert Bensch, Özgün Çiçek, Ahmed Abdulkadir, Yassine Marrakchi, Anton Böhm,

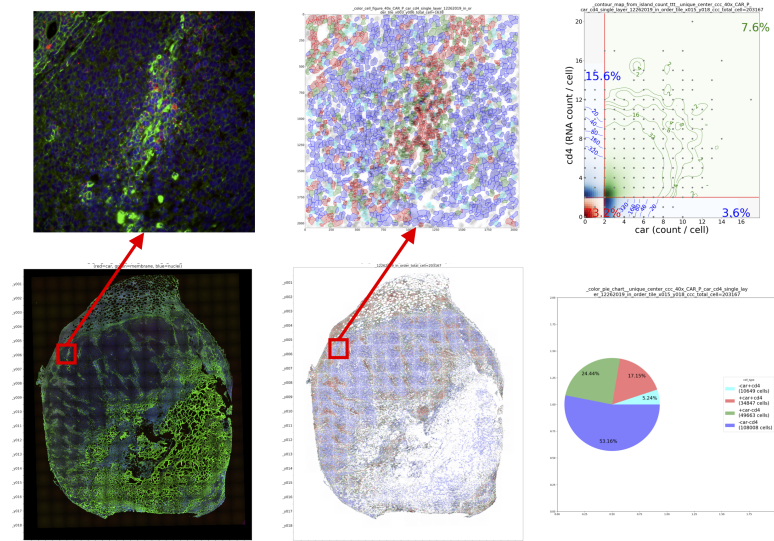


Figure 6. Cell phenotype analysis of 4-plex immuno-fluorescent tissue image stained by 4 biomarkers: CAR, CD4, nuclei, and membrane. The left panel is the raw stitched cancer tissue. The central panel is profiling map of 4 phenotypes from RRSCell inferencing. The right panel is corresponding pie chart and the contour map with the gating condition of captured mRNA contents of individual cells from the whole slide tissue.

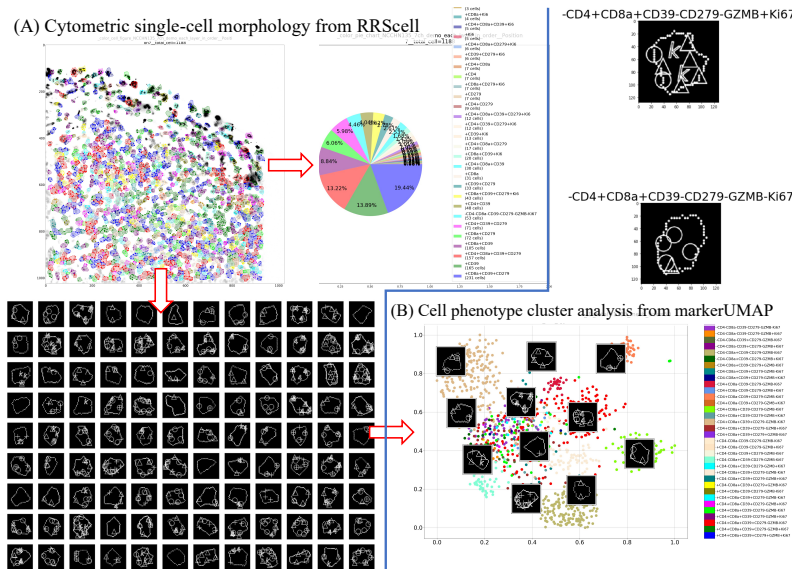


Figure 7. RRSCell phenotype detection of 7-plex immuno-fluorescent image from cancer tissue stained by 7 biomarkers: CD4, CD8a, CD39, CD279, DAPI, GZMB, and Ki67. (A) Demonstration of extracting single-cell level information from individual cells in one corner of whole slide of tissue by RRSCell. The pie-chart illustrates that a total of 34 cell-phenotypes are detected in the demo image. (B) Demonstration of cell phenotype cluster analysis by markerUMAP tool.

Jan Deubner, Zoe Jäckel, Katharina Seiwald, Alexander Dovzhenko, Olaf Tietz, Cristina Dal Bosco, Sean Walsh, Deniz Saltukoglu, Tuan Leng Tay, Marco Prinz, Klaus Palme, Matias Simons, Ilka Diester, Thomas Brox, and Olaf Ronneberger. U-net: deep learning for cell counting, detection, and morphometry. *Nature Methods*, 16(1):67–70, 2019.

[6] Rihuan Ke, Aurélie Bugeau, Nicolas Papadakis, Peter Schuetz, and Carola-Bibiane Schönlieb. Learning to seg-

ment microscopy images with lazy labels. In Adrien Bartoli and Andrea Fusiello, editors, *Computer Vision –ECCV 2020 Workshops*, pages 411–428, Cham, 2020. Springer International Publishing.

[7] Alvason Zhenhua Li, Lawrence Corey, and Jia Zhu. Random-reaction-seed method for automated identification of neurite elongation and branching. *Scientific Reports*, 9(1):2908, 2019.

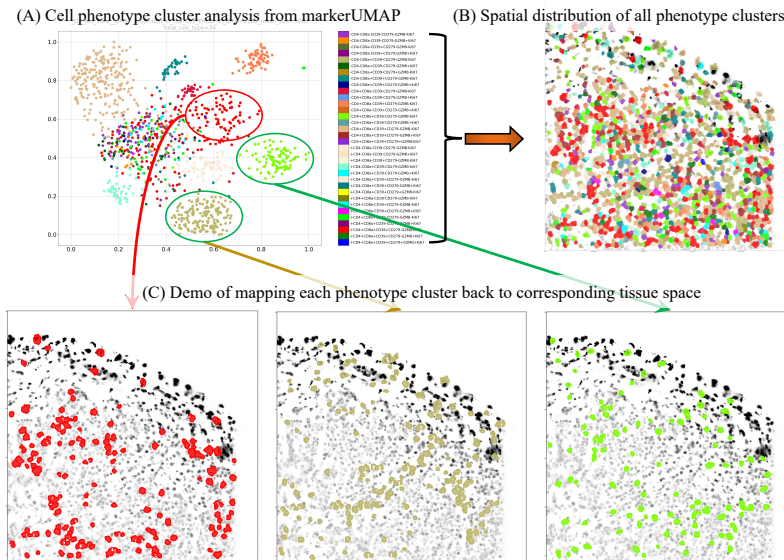


Figure 8. Demo of spatial analysis of high dimensional multiplexed images from cancer tissue stained by 7 biomarkers: CD4, CD8a, CD39, CD279, DAPI, GZMB, and Ki67. (A) is the cell phenotype cluster analysis by markerUMAP. (B) is spatial distribution of all phenotype clusters. (C) are demonstrations of mapping each phenotype cluster back to corresponding tissue space.

- [8] Leland McInnes and John Healy. Umap: Uniform manifold approximation and projection for dimension reduction. *arXiv*, 2018.
- [9] Olaf Ronneberger, Philipp Fischer, and Thomas Brox. U-net: Convolutional networks for biomedical image segmentation. *arXiv*, 2015.
- [10] Denis Schapiro, Hartland W Jackson, Swetha Raghuraman, Jana R Fischer, Vito R T Zanutelli, Daniel Schulz, Charlotte Giesen, Raúl Catena, Zsuzsanna Varga, and Bernd Bodenmiller. histocat: analysis of cell phenotypes and interactions in multiplex image cytometry data. *Nature Methods*, 14(9):873–876, 2017.
- [11] Caleb R. Stoltzfus, Jakub Filipek, Benjamin H. Gern, Brandy E. Olin, Joseph M. Leal, Yajun Wu, Miranda R. Lyons-Cohen, Jessica Y. Huang, Clarissa L. Paz-Stoltzfus, Courtney R. Plumlee, Thomas Pöschinger, Kevin B. Urdahl, Mario Perro, and Michael Y. Gerner. Cytomap: A spatial analysis toolbox reveals features of myeloid cell organization in lymphoid tissues. *Cell Reports*, 31(3):107523, 2020.
- [12] Daniel Stone, Kelly R. Long, Michelle A. Loprieno, Harshana S. De Silva Feelixge, Elizabeth J. Kenkel, R. Matt Liley, Stephen Rapp, Pavitra Roychoudhury, Thuy Nguyen, Laurence Stensland, Rossana Colón-Thillet, Lindsay M. Klouser, Nicholas D. Weber, Connie Le, Jessica Wagoner, Erin A. Goecker, Alvason Zhenhua Li, Karsten Eichholz, Lawrence Corey, D. Lorne Tyrrell, Alexander L. Greninger, Meei-Li Huang, Stephen J. Polyak, Martine Aubert, John E. Sagartz, and Keith R. Jerome. Crispr-cas9 gene editing of hepatitis b virus in chronically infected humanized mice. *Molecular Therapy - Methods & Clinical Development*, 20:258–275, 2021.
- [13] Wei Chang Colin Tan, Sanjna Nilesh Nerurkar, Hai Yun Cai, Harry Ho Man Ng, Duoduo Wu, Yu Ting Felicia Wee, Jeffrey Chun Tatt Lim, Joe Yeong, and Tony

Kiat Hon Lim. Overview of multiplex immunohistochemistry/immunofluorescence techniques in the era of cancer immunotherapy. *Cancer Communications*, 40(4):135–153, 2021/03/13 2020.